

Extension of the energy range of the moveable fast ion probe on TFTR

D. S. Darrow, R. L. Boivin,^{a)} and S. J. Zweben
Princeton University, Plasma Physics Laboratory, Princeton, New Jersey 08543

(Presented on 16 March 1992)

The range of detectable energies of the moveable fast ion probe on TFTR has been extended by the removal of a 3- μm Al foil across its entrance aperture. This foil formerly stopped hydrogenic ions with energies below 300 keV, and helium ions with energies below 900 keV. The new arrangement allows detection of neutral beam ions (100-keV D^+) at toroidal fields between 1 and 5 T. Data typical of the probe's enhanced performance are shown.

I. INTRODUCTION

The Tokamak Fusion Test Reactor (TFTR) is equipped with four probes which provide information on the losses of MeV ions, typically the fusion products p (3 MeV), t (1 MeV), and ^4He (3.5 and 3.7 MeV).¹ Such measurements have allowed assessment of various processes that might expel alpha particles and hence affect the energy balance in an ignited tokamak.^{2,3} Three of the probes are fixed in position, and measure the losses at poloidal angles of -45° , -60° , and -90° . The fourth probe is moveable in the major radial direction and is located at a poloidal angle of -20° . This probe has been used to measure stochastic ripple diffusion of charged fusion products.⁴

Since its installation in 1989, the moveable fast ion probe has included a 3- μm -thick aluminum foil placed across its aperture, as have all the stationary probes. The foil has excluded protons, deuterons, and tritons with energies below 300 keV, and helium ions with energies below 900 keV.⁵ This work describes the enhancement of the probe's performance which has been obtained by removing the foil so that lower energy particles may be detected.

II. DESCRIPTION OF THE PROBE

Figure 1 shows schematically the principal of operation of the probe. Ions of sufficiently large gyroradius can enter the probe through the aperture and slit, and then strike the scintillator, creating light. The position at which the scintillator is illuminated indicates the gyroradius and pitch angle of the incident ion. The intensity of the light from the scintillator is assumed to be linearly proportional to both the particle flux and the energy of the particles^{4,6} for the present fluxes. A set of lenses focuses the image of the scintillator onto a fiber optic bundle outside the vacuum vessel. The bundle then carries the image to a detector in the basement of the TFTR complex, where it is recorded by an intensified video camera. A beamsplitter and lens focus a fraction of the total light from the scintillator onto a photomultiplier tube, which provides a total intensity measurement with a time response faster than that possible with the videocamera. This feature has proven valuable in fluctuation studies.

The useful area of the scintillator within the probe is 2.2 cm \times 2.2 cm. The probe front aperture is 1 mm \times 2 mm. The aperture and scintillator are mounted upon a box of square cross section, 3.2 cm along a side and 17.8-cm high. The box assembly is protected from damage by the plasma with a carbon-fiber-composite shield that is cylindrical in shape and which has an o.d. of 6.4 cm. A tapered hole in the shield allows ions to enter the aperture, 2.9 cm from the tip of the shield. The useful range of probe motion is between aperture positions of $R=3.62$ m and $R=3.38$ m (in major radius). At major radii larger than 3.62 m, the aperture is behind the protective plates on the wall of the TFTR vessel, and no ions can reach it. For $R < 3.525$ m, the aperture is no longer shadowed by the rf limiter (the limiter closest to the plasma at this poloidal angle). The range of positions that can be scanned is, therefore, 14.5 cm beyond the rf limiter, and 9.5 cm in its shadow.

III. MODIFICATION OF THE PROBE

In preparation for the 1991 campaign, the 3- μm aluminum foil mentioned above was removed from the moveable probe so that lower energy ions could be detected. Without this foil, the minimum detectable ion energy is limited by the geometry of the probe—the gyroradius must be sufficiently large that the particle can pass through both

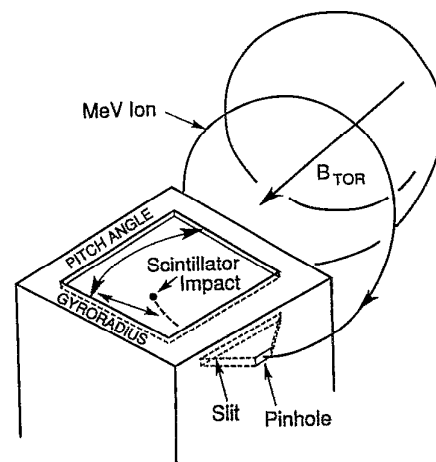


FIG. 1. Schematic of the fast ion probe and its operation.

^{a)}Present address: Plasma Fusion Center, Massachusetts Institute of Technology, Cambridge, MA 02139.

the aperture and the slit. This requires that the gyroradius, ρ , equal or exceed 1.2 cm, which sets a lower energy limit of

$$E_{\min} = \frac{0.012q_i^2 B_T^2}{m_i \sin^2 \chi},$$

in MKS units, where q_i is the ion charge, m_i is the ion mass, B_T is the toroidal field, and χ is the pitch angle with respect to the toroidal field, $\chi = \arccos(v_{\text{tor}}/v)$.

The amount of light emitted per particle impact is, to a good approximation, proportional to the particle's energy, provided the range of the particle in the scintillator is less than its thickness ($\sim 10 \mu\text{m}$). The exact efficiency (light output per particle energy input) depends upon the scintillator used, but is typically 12% for ZnS(Ag) (EIA phosphor P11), and 7% for ZnS(Cu) (EIA phosphor P31),⁷ the two phosphors most favored for this application because of their brightness and fast time response. Light emission for 3-MeV protons incident upon the scintillator is proportional to the flux of incident particles up to $\sim 10^{10} \text{cm}^{-2} \text{s}^{-1}$. Above this flux, light emission begins to saturate.⁶ The saturation flux for 100-keV deuterons incident upon these scintillators has not been determined yet.

Because the light from beam ions in the detector has often been observed to be much larger than that of the tritons and protons, there was initially some concern that charge accumulation on the scintillator surface might artificially enlarge the luminous spot produced by beam ions. In fact, absolute intensity calibration of the system indicates that the beam ion flux results in a current density to the scintillator surface of about 10^{-8}amp/cm^2 which is typical of the average current densities striking the phosphor in a cathode ray tube, for which charge accumulation on the phosphor is not sufficient to affect operation. Even so, the scintillator that will be used during the 1992 campaign will incorporate a metallized substrate, so that any charge that does accumulate will be more readily drained.

IV. EXPERIMENTAL RESULTS

A. Background light

The removal of the $3\text{-}\mu\text{m}$ foil potentially allows light to enter the probe housing from the plasma, and there was some concern that this light might scatter within the housing and cause a substantial increase in the background signal. There is, in fact, no direct line of sight from the plasma to the scintillator surface, and operation of the probe during the 1991 campaign revealed no increase in the background signal due to plasma light. The signal level during operation in ohmic plasmas (which lack significant densities of fast ions, but which still produce light) is not detectably different from the level seen during shots in which no plasma is formed at all.

B. 100-keV beam ions

Figure 2(a) shows the video camera signal from a low toroidal field, beam-injected plasma. Depicted are contours of constant luminosity, with the superimposed grid of

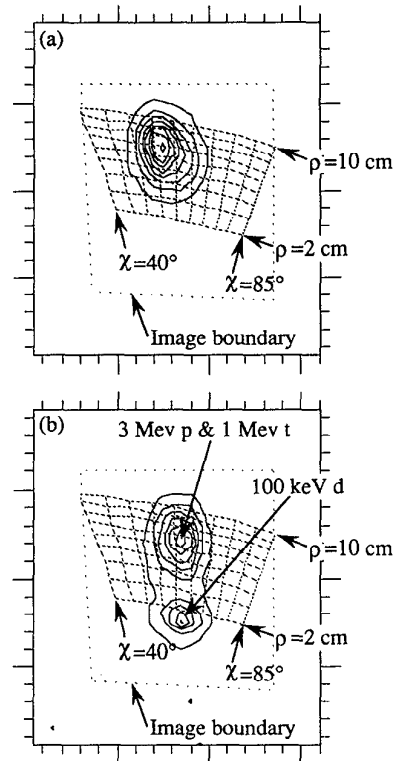


FIG. 2. Videocamera images of the scintillator. (a) 100-keV deuterium beam ions in a 1.1-T toroidal field at $R=3.40 \text{ m}$. (shot 62385). (b) 100-keV deuterium beam ions, 1-MeV tritons, and 3-MeV protons in a 3.5-T toroidal field at $R=3.42 \text{ m}$ (shot 60331).

gyroradius and pitch angle space. These data were taken with the probe at $R=3.40 \text{ m}$, 0.125 m inside the rf limiter, at which location the toroidal field strength was 1.09 T. The gyroradius for 100-keV beam ions should then be 5.9 cm. The broad instrumental response function of approximately $\pm 1 \text{ cm}$ is due to the relatively wide slits, the poor resolution of the fiber optic bundle system, and the fact that orbits strike the surface of the scintillator at shallow angles. The detected feature has maximum intensity at 6.8 cm, which agrees with the predicted gyroradius within the noted uncertainty.

The feature cannot be attributed to fusion product ions for two reasons: first, the gyroradius of such ions would have been 25 cm, considerably larger than observed. In addition, the time-history of the feature, like that shown in Fig. 3(b), indicates a very sudden reduction in the source of these particles at the end of beam injection. In contrast, fusion products would continue to be created and lost for several hundred milliseconds after the end of NBI (see Sec. C, below). Therefore, this feature is due to neutral beam ions at or near their full injection energy.

C. 1-MeV tritons and 3-MeV protons

Figure 2(b) shows the detector image during a discharge with high toroidal field, 4.9 T on axis. In this case, features from two distinct classes of ions are seen. The low

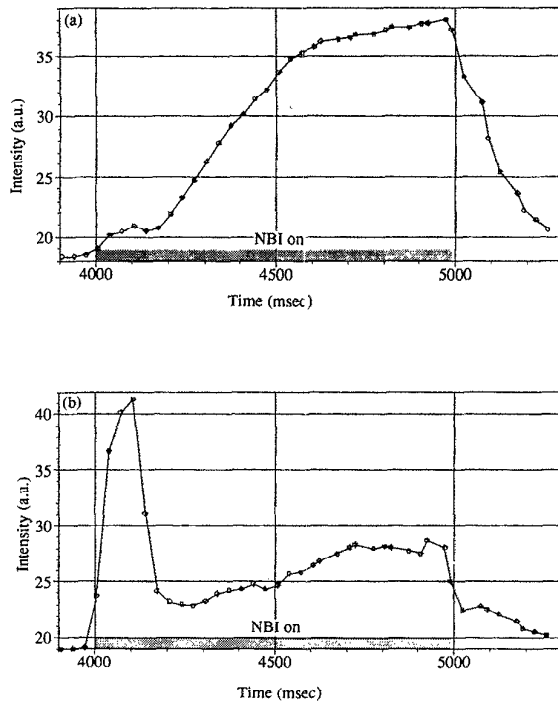


FIG. 3. Time histories of the two features depicted in Fig. 2(b). (a) Intensity vs time for the $\rho=7$ cm feature. (b) Intensity vs time for the $\rho=1.6$ cm feature.

gyroradius feature is at 1.6 cm, with a pitch angle of $\chi=62^\circ$, while the large gyroradius feature is at 7.0 cm, and a pitch angle also of $\chi=62^\circ$. The probe aperture was at $R=3.42$ m, and the computed gyroradius of 100-keV beam ions is 1.8 cm, in agreement with the lower feature. Protons and tritons from fusion reactions would appear at $\rho=7.1$ cm, in accord with the upper feature's position. Figure 3 supports this identification of the features. In Fig. 3(a), the intensity of a region centered on the $\rho=7.0$ cm spot is plotted versus time. The decay over several tenths of a second at the end of beam injection is indicative of the

gradual loss of the source of fusion products as the remaining beam ions slow down. The trace in Fig. 3(b) falls more abruptly at the end, coincident with the removal of the source of beam ions. Because of the broad instrumental function, there is some crosstalk between the two traces, as seen in the behavior of their baselines.

These figures show the ability of the probe to detect beam ion losses even at full toroidal field.

D. ICRF ions

The probe has been inserted into the vessel during H-minority ICRF experiments. In such experiments, several effects have been noted. In some discharges, the fusion product spot shows a factor of two enhancement of the loss during ICRF. In others, separate features appear on the detector during ICRF, presumably due to high-energy ions in the rf-driven tail. These will be the subject of future investigations.

V. SUMMARY

The moveable midplane fast ion probe on TFTR has been modified so that it can detect ions with energies below its previous cutoff. No added technical problems have occurred with this enhancement. The change has allowed observation of beam ion losses under a variety of experiments ranging from low field to high field.

ACKNOWLEDGMENTS

This work was performed under U.S. Department of Energy contract No. DE-AC02-76-CHO-3073.

¹S. Zweben *et al.*, *Rev. Sci. Instrum.* **60**, 576 (1989).

²S. J. Zweben *et al.*, *Nucl. Fusion* **30**, 1551 (1990).

³S. J. Zweben *et al.*, *Nucl. Fusion* **31**, 2219 (1991).

⁴R. L. Boivin, Ph.D. Thesis, Princeton University, 1991.

⁵H. H. Anderson and J. F. Ziegler, in *The Stopping and Ranges of Ions in Matter*, edited by J. F. Ziegler (Pergamon, New York, 1977), Vol. 3; U. Littmark and J. F. Ziegler, in *The Stopping and Ranges of Ions in Matter*, edited by J. F. Ziegler (Pergamon, New York, 1980), Vol. 6.

⁶M. Tuzsewski *et al.*, these proceedings.

⁷Phosphor Resource Manual for Industrial and Military Cathode Ray Tubes, Imaging and Sensing Technology Corporation, Horseheads, NY.